JOURNAL OF THE AMERICAN COLLEGE OF CARDIOLOGY
VOL. 68, NO. 17, 2016
ISSN 0735-1097
http://dx.doi.org/10.1016/j.jacc.2016.07.766

PITX2 Modulates Atrial Membrane Potential and the Antiarrhythmic Effects of Sodium-Channel Blockers

Fahima Syeda, PhD,[a] Andrew P. Holmes, PhD,[a] Ting Y. Yu, PhD,[a,b] Samantha Tull, PhD,[a] Stefan Michael Kuhlmann, BSc,[a] Davor Pavlovic, DPhil,[a] Daniel Betney, BMedSc, MBBS,[a] Genna Riley, DPhil,[a] Jan P. Kucera, MD,[c] Florian Jousset, PhD,[c] Joris R. de Groot, MD,[d] Stephan Rohr, MD,[c] Nigel A. Brown, PhD,[e] Larissa Fabritz, MD,[a,f,g,h] Paulus Kirchhof, MD[a,f,g,h,i]

ABSTRACT

BACKGROUND Antiarrhythmic drugs are widely used to treat patients with atrial fibrillation (AF), but the mechanisms conveying their variable effectiveness are not known. Recent data suggested that paired like homeodomain-2 transcription factor (*PITX2*) might play an important role in regulating gene expression and electrical function of the adult left atrium (LA).

OBJECTIVES After determining LA *PITX2* expression in AF patients requiring rhythm control therapy, the authors assessed the effects of *Pitx2c* on LA electrophysiology and the effect of antiarrhythmic drugs.

METHODS LA *PITX2* messenger ribonucleic acid (mRNA) levels were measured in 95 patients undergoing thoracoscopic AF ablation. The effects of flecainide, a sodium (Na^+)-channel blocker, and d,l-sotalol, a potassium channel blocker, were studied in littermate mice with normal and reduced *Pitx2c* mRNA by electrophysiological study, optical mapping, and patch clamp studies. *PITX2*-dependent mechanisms of antiarrhythmic drug action were studied in human embryonic kidney (HEK) cells expressing human Na channels and by modeling human action potentials.

RESULTS Flecainide 1 μmol/l was more effective in suppressing atrial arrhythmias in atria with reduced *Pitx2c* mRNA levels (*Pitx2c*$^{+/-}$). Resting membrane potential was more depolarized in *Pitx2c*$^{+/-}$ atria, and TWIK-related acid-sensitive K^+ channel 2 (TASK-2) gene and protein expression were decreased. This resulted in enhanced post-repolarization refractoriness and more effective Na-channel inhibition. Defined holding potentials eliminated differences in flecainide's effects between wild-type and *Pitx2c*$^{+/-}$ atrial cardiomyocytes. More positive holding potentials replicated the increased effectiveness of flecainide in blocking human $Na_v1.5$ channels in HEK293 cells. Computer modeling reproduced an enhanced effectiveness of Na-channel block when resting membrane potential was slightly depolarized.

CONCLUSIONS *PITX2* mRNA modulates atrial resting membrane potential and thereby alters the effectiveness of Na-channel blockers. *PITX2* and ion channels regulating the resting membrane potential may provide novel targets for antiarrhythmic drug development and companion therapeutics in AF. (J Am Coll Cardiol 2016;68:1881–94) © 2016 The Authors. Published by Elsevier on behalf of the American College of Cardiology Foundation. This is an open access article under the CC BY license (http://creativecommons.org/licenses/by/4.0/).

Listen to this manuscript's audio summary by *JACC* Editor-in-Chief Dr. Valentin Fuster.

From the [a]Institute of Cardiovascular Sciences, University of Birmingham, Birmingham, United Kingdom; [b]Physical Sciences of Imaging in the Biomedical Sciences, School of Chemistry, University of Birmingham, Birmingham, United Kingdom; [c]Department of Physiology, University of Bern, Bern, Switzerland; [d]Heart Center, Department of Cardiology, Academisch Medisch Centrum, Amsterdam, the Netherlands; [e]St. George's Hospital Medical School, University of London, London, United Kingdom; [f]Department of Cardiovascular Medicine, University Hospital Muenster, Muenster, Germany; [g]Atrial Fibrillation NETwork, Muenster, Germany; [h]University Hospitals Birmingham NHS Foundation Trust, Birmingham, United Kingdom; and the [i]Sandwell and West Birmingham Hospitals NHS Trust, Birmingham, United Kingdom. This work was supported by the European Union (EUTRAF 25105 to Drs. Kirchhof and Rohr; and Grant Agreement No. 633196 [CATCH ME] to Drs. Kirchhof and Fabritz); British Heart Foundation (FS/13/43/30324 to Drs. Kirchhof and Fabritz); Leducq Foundation to Dr. Kirchhof; Physical Science of Imaging in Biomedical Sciences (PSIBS) University of Birmingham for TY to Dr. Fabritz (EP/F50053X/1); DFG (FA 413 3/1) to Dr. Fabritz; Swiss National Science Foundation (138297) to Dr. Rohr; and Boehringer Ingelheim Foundation to Mr. Kuhlmann. Dr. de Groot is supported by

ABBREVIATIONS AND ACRONYMS

AAD = antiarrhythmic drug

APD = action potential duration

ERP = effective refractory period

HEK = human embryonic kidney

LA = left atrium

LAA = left atrial appendage

mRNA = messenger ribonucleic acid

Na = sodium

PITX2 = paired like homeodomain-2

PRR = post-repolarization refractoriness

RMP = resting membrane potential

SNP = single nucleotide polymorphism

TASK-2 = TWIK-related acid-sensitive K^+ channel

Atrial fibrillation (AF) causes cardiovascular death, frequent hospitalization, and cognitive decline even in patients treated according to guidelines (1–3). Antiarrhythmic drug (AAD) therapy remains the most commonly used treatment to maintain sinus rhythm in AF patients, but AAD effectiveness remains limited (3). Unfortunately, we lack a basic understanding of why AADs prevent AF over long periods in some patients but not in others (4,5). Identifying factors that modify the effects of AADs would allow the selection of responsive patients and could help guide development of novel AADs (6).

Paired like homeodomain-2 transcription factor (*PITX2*) is a transcription factor that regulates the development of the left atrium (LA) and thoracic organs. Its c isoform is expressed in the adult LA and regulates the expression of LA ion channels (7–9). Low atrial *Pitx2* expression renders mice susceptible to AF and shortens the LA action potential (8,10,11). In this study, we investigated how atrial *PITX2* modifies the effects of AADs.

SEE PAGE 1895

We detected variable LA *PITX2* messenger ribonucleic acid (mRNA) expression in AF patients requiring rhythm control therapy. After finding that low *Pitx2c* enhanced the effect of flecainide, mediated by a more positive resting membrane potential (RMP), we identified reduced TWIK-related acid-sensitive K^+ channel 2 (TASK-2) expression as a possible driver of this effect and replicated these effects in cells expressing human sodium (Na) channels and in a human atrial action potential model.

METHODS

All experiments were conducted under the Animals (Scientific Procedures) Act 1986, and approved by the home office (PPL number 30/2967) and the institutional review board at the University of Birmingham. Analyses of human atrial tissue were approved by the institutional review board of Academic Medical Center, Amsterdam, the Netherlands. All patients provided written informed consent.

Left atrial appendages (LAAs) were excised from 95 patients undergoing bilateral thoracoscopic AF ablation either in the AFACT (Atrial Fibrillation Ablation and Autonomic Modulation via Thoracoscopic Surgery) trial (12) or undergoing similar procedures in the same centers using an endoscopic stapling device, snap frozen in liquid nitrogen and stored at -80°C (13). Deoxyribonucleic acid and ribonucleic acid were extracted using DNeasy and RNeasy kits (Qiagen Ltd., Manchester, United Kingdom), respectively. *PITX2* mRNA content was quantified by quantitative polymerase chain reaction. Single nucleotide polymorphisms (SNPs) rs2200733, rs6838973, and rs1448818 (14) were identified using TaqMan assays (Thermo Fisher Scientific Inc., Waltham, Massachusetts).

Adult mice (age 12 to 16 weeks) on an MF1 background with normal or reduced ($Pitx2c^{+/-}$) atrial *Pitx2c* expression were studied (8).

LA epicardial monophasic action potentials were recorded from Langendorff-perfused murine hearts (8,15). Programmed stimulation was performed at baseline and with flecainide 1 μmol/l or d,l-sotalol 10 μmol/l. Arrhythmia inducibility and effective refractory period (ERP) were measured by using single right atrial extrastimuli after steady-state pacing in 1-ms decrements (15–18). Transmembrane action potentials were recorded using borosilicate glass microelectrodes from superfused murine LAs (17), RMP, action potential duration (APD), upstroke velocity, and activation times were analyzed (15,17,18).

The human atrial cell model of Courtemanche et al. (19) was used. $Pitx2c^{+/-}$ deficiency was modeled by reducing I_{K1} conductance by 25% and doubling I_{Kr} conductance. Simulations were run in strands of 100 atrial cells (cell length 100 μm). The 5 leftmost cells of the strand were paced (S1) for 2 min at 1,000- and 500-ms basic cycle lengths. Premature stimulation (S2) was applied to determine the ERP and conduction velocity as measured from cells 25 to 75. Values for all other parameters were measured from the 50th cell. For the modeling, post-repolarization

NWO/ZonMW VIDI Grant 016.146.310. Dr. Riley is currently employed by Bio-Techne (R&D Products). Dr. Fabritz has received further institutional research grant support from DFG, MRC, and Gilead Inc. Dr. Kirchhof has received further research support from the German Centre for Heart Research and from several drug and device companies active in atrial fibrillation; and has received honoraria from several such companies. Drs. Syeda, Fabritz, and Kirchhof are listed as inventors on a patent (WO2015/140571) held by the University of Birmingham on genotype-specific antiarrhythmic drug therapy of atrial fibrillation. All other authors have reported that they have no relationships relevant to the contents of this paper to disclose. Drs. Syeda and Holmes contributed equally to this work.

Manuscript received February 11, 2016; revised manuscript received July 5, 2016, accepted July 20, 2016.

refractoriness (PRR) was calculated as the difference between APD at -60 mV repolarization and ERP.

LA cell isolation was performed as previously reported (20). Standard I_{Na} and I_{K1} currents were recorded as previously published (18–20). Background K^+ (TASK-like) currents sensitive to high Ba^{2+} (10 mM) were measured (21–23). Human embryonic kidney (HEK) 293 cells stably expressing the human $Na_v1.5$ channel were obtained (SB Ion Channels, Glasgow, UK).

Ribonucleic acid and complementary deoxyribonucleic acid were synthesized from murine LA, (SuperScript VILO, Thermo Fisher Scientific Inc.) to quantify expression of 20 atrial ion channels and genes with suspected *PITX2*-dependent regulation (9) using custom-designed Taqman low density array plates (Thermo Fisher Scientific Inc.). Western immunoblotting was performed on murine LA tissue lysates with antibodies detecting TASK-2, $K_v1.6$, Na/K ATPase alpha-1, Na/K ATPase alpha-2, Na/Ca exchanger 1, Serca2a, $Na_v1.5$, or calnexin, using standard methods.

Optical action potentials and calcium ion (Ca^{2+}) transients were recorded in murine LA and analyzed using custom-made MATLAB algorithms (MathWorks, Natick, Massachusetts) as previously described (17).

STATISTICAL ANALYSIS. All experiments were performed and analyzed in a blinded fashion. Murine studies were performed and analyzed blinded to genotype in littermate pairs. Categorical data were compared using the Fisher exact test. Numerical data were compared by 2-sided paired parametric Student *t* tests (e.g., measurements before and after perfusion of flecainide or sotalol) and Wilcoxon signed rank tests. Multiple measurements were assessed by repeated measures of analysis of variance followed by correction for multiple comparison (Bonferroni test) if the overall test was significant. Two-sided $p < 0.05$ were considered significant. Box plots depict individual measurements (points), mean, and SEM. Statistics and figures were created using Prism 5 (GraphPad Software, San Diego, California).

RESULTS

PITX2 mRNA varied markedly in human LAA (**Central Illustration**) harvested from AF patients (**Table 1**) (13), suggesting that a 50% lowered *PITX2* expression defines a large, potentially clinically relevant group of AF patients. This did not directly correlate with SNP haplotype (**Table 2**), although we found numerically lower *PITX2c* levels in patients with 5 risk alleles.

Flecainide suppressed atrial arrhythmias in murine *Pitx2c*$^{+/-}$ hearts. Flecainide abolished induced atrial arrhythmias in hearts with reduced *Pitx2c* expression (0 of 17 hearts with atrial arrhythmias) but not in hearts with normal *Pitx2c* expression (atrial arrhythmias remained in 3 of 12 hearts) (**Figures 1A to 1C**).

TABLE 1 Baseline Characteristics (N = 101)*

Age, yrs	59.7 ± 8.4 (40-76)
Male	79
Congestive heart failure	6
Hypertension	34
Age ≥75 yrs	1
Diabetes	9
Stroke/transient ischemic attack/embolus	10
Vascular disease	10
Female	22
Age ≥65 yrs	31
CHA_2DS_2-VASc score	
0	60
1	24
≥2	17
Previous catheter ablation for AF	20
Type of AF	
Paroxysmal	44
Persistent	56
Longstanding persistent	1
AF duration, yrs	6.0 (1-35)
Antiarrhythmic drugs and rate control agents	
Quinidine or disopyramide	4
Flecainide or propafenone	33
Amiodarone, dronedarone, or sotalol	41
Beta blockers	53
Verapamil or diltiazem	17
Digoxin	15
Anticoagulant agents (before PVI procedure)	
Vitamin K antagonists	89
Antiplatelets	6

Values are mean ± SD (range), n, or mean (range). *Left atrial appendages were collected from these patients with atrial fibrillation (AF).
PVI = pulmonary vein isolation.

TABLE 2 *PITX2* mRNA Expression in Left Atrial Appendages From AF Ablation Patients*

Risk Alleles	25% IQR	Median	75% IQR	Mean	SEM	No. of Patients
0	3.22	3.69	5.22	4.04	0.6	3
1	2.96	4.25	6.25	4.54	0.5	13
2	2.65	3.78	4.75	3.94	0.3	22
3	2.74	3.72	4.92	3.83	0.4	17
4	3.00	4.29	5.41	4.39	0.5	10
5	1.96	2.66	4.66	3.10	0.7	4
6	4.95	4.95	4.95	4.95	0.0	1

*This dataset was grouped according to the number of risk single nucleotide polymorphism (SNP) alleles for AF on chromosome 4q25 (rs2200733, SNP2 rs6838973, rs1448818 [13]). Although *PITX2* mRNA is numerically lower in patients with 5 or 6 risk alleles, we did not find a *PITX2* mRNA gradient according to AF risk.
IQR = interquartile range; LA = left atrium; other abbreviations as in Table 1.

FIGURE 1 Atrial Arrhythmia Inducibility in *Pitx2c*$^{+/-}$ Murine Whole Hearts

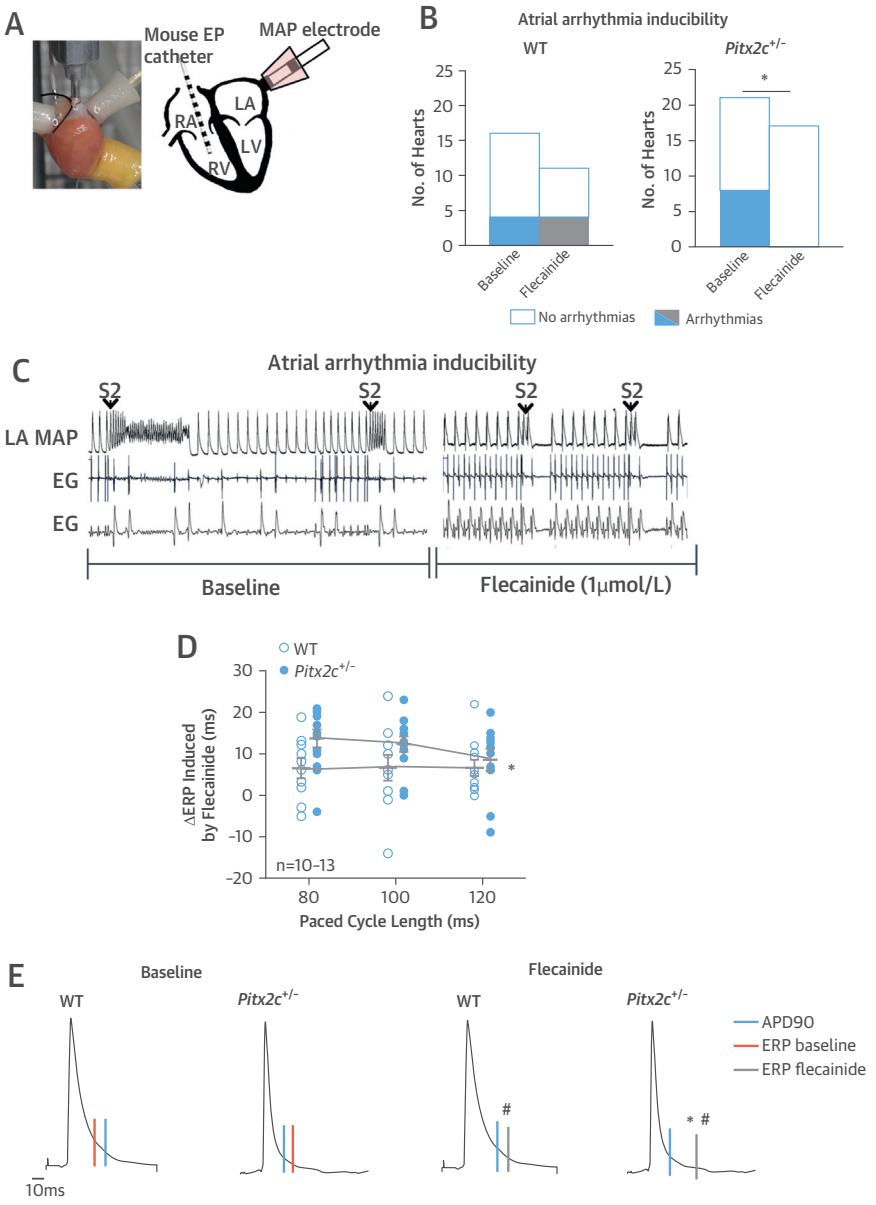

(A) Image and schematic representation of the Langendorff-perfused heart. **(B)** Atrial arrhythmia inducibility in isolated, beating hearts from wild-type (WT) and reduced paired like homeodomain 2 messenger ribonucleic acid (*Pitx2c*$^{+/-}$) mice. Flecainide abolished atrial arrhythmia inducibility in *Pitx2c*$^{+/-}$ hearts only. *$p < 0.05$ flecainide versus baseline. **(C)** Representative trace of atrial fibrillation (AF) induced during programmed stimulation at baseline, showing reduced severity of arrhythmias with 1 μmol/l flecainide in *Pitx2c*$^{+/-}$ atria. **(D)** Effects of flecainide on atrial effective refractory period (ERP) in wild-type and *Pitx2c*$^{+/-}$ isolated, beating hearts. Shown is the difference in atrial ERP between baseline and 1 μmol/l flecainide at 80- to 120-ms paced cycle length following a single extrastimulus (S2) in WT and *Pitx2c*$^{+/-}$ isolated, beating hearts. *$p < 0.05$ between genotypes across all cycle lengths. **(E)** Whereas flecainide prolonged ERP in both genotypes, this effect was more pronounced in *Pitx2c*$^{+/-}$ atria. Flecainide caused post-repolarization refractoriness (PRR), the difference between ERP **(orange and grey lines)** and APD_{90} **(blue lines)**, in WT and *Pitx2c*$^{+/-}$ atria. Flecainide-induced PRR in *Pitx2c*$^{+/-}$ is almost 3 times that of WT atria. *$p < 0.05$ WT versus *Pitx2c*$^{+/-}$. #$p < 0.05$ baseline versus 1 μmol/l flecainide. APD = action potential duration; EG = intracardiac electrogram; EP = electrophysiology; LA = left atrium; LV = left ventricle; MAP = monophasic action potential; RA = right atrium; RV = right ventricle.

TABLE 3 Effect of Flecainide on Refractoriness and Repolarization in Mouse Hearts

Paced CL, ms	Wild-Type						*Pitx2c*$^{+/-}$					
	120		100		80		120		100		80	
	Baseline	Flecainide	Baseline	Flecainide	Baseline	Flecainide	Baseline	Flecainide	Baseline	Flecainide	Baseline	Flecainide
LA ERP, ms												
	23.5 ± 2.3 (11)	29.8 ± 3.0 (11)	22.2 ± 2.1 (11)	29.6 ± 3.3 (11)	21.9 ± 2.4 (10)	28.7 ± 3.5* (10)	30.5 ± 2.4 (11)	38.5 ± 3.3* (11)	28.0 ± 2.3 (13)	40.2 ± 2.8* (13)	27.5 ± 2.5 (13)	41.2 ± 3.0*† (13)
LA monophasic APD, ms												
APD_{50}	10.2 ± 1.3 (8)	14.5 ± 1.7 (8)	10.8 ± 1 (8)	11.9 ± 1.6 (8)	10.4 ± 0.7 (7)	12.0 ± 1.1 (7)	12.4 ± 1.1 (15)	14.4 ± 1.3 (15)	11.5 ± 1.0 (15)	12.4 ± 1.1 (15)	10.6 ± 0.9 (11)	10.3 ± 1.0 (11)
APD_{70}	17.8 ± 2.2 (9)	23 ± 2.1 (9)	18.4 ± 1.6 (9)	18.7 ± 2.2 (9)	18.1 ± 1.2 (8)	18.1 ± 1.9 (8)	18.0 ± 1.6 (15)	19.2 ± 1.8 (15)	16.0 ± 1.4 (13)	16.2 ± 1.4 (13)	14.9 ± 1.0† (10)	13.1 ± 0.7 (10)
APD_{90}	31.3 ± 3.0 (8)	37.4 ± 2.8 (8)	31.5 ± 2.5 (9)	29.9 ± 2.9 (9)	31.0 ± 1.4 (8)	28.4 ± 2.7 (8)	28.3 ± 2.2 (13)	29.9 ± 2.2 (13)	27.4 ± 2.2 (13)	26.6 ± 1.5 (13)	26.8 ± 1.7 (10)	23.1 ± 1.4 (10)
LA transmembrane APD, ms												
APD_{30}	4.5 ± 0.1 (30)	5.5 ± 0.3 (22)	4.5 ± 0.1 (30)	5.4 ± 0.3 (22)	4.4 ± 0.1 (30)	5.2 ± 0.3 (22)	4.0 ± 0.1 (31)	4.7 ± 0.2 (24)	3.9 ± 0.1 (31)	4.6 ± 0.2 (24)	3.8 ± 0.1† (31)	4.4 ± 0.2 (24)
APD_{50}	6.7 ± 0.2 (30)	8.2 ± 0.5 (22)	6.6 ± 0.2 (30)	8.0 ± 0.4 (22)	6.4 ± 0.2 (30)	7.8 ± 0.5 (22)	5.9 ± 0.2 (31)	7.1 ± 0.4 (24)	5.7 ± 0.2 (31)	7.0 ± 0.4 (24)	5.6 ± 0.2† (31)	6.7 ± 0.3 (24)
APD_{70}	10.5 ± 0.4 (30)	12.7 ± 0.8 (22)	10.1 ± 0.4 (30)	12.1 ± 0.7 (22)	9.6 ± 0.4 (30)	11.8 ± 0.7 (22)	8.9 ± 0.4 (31)	10.7 ± 0.6 (24)	8.6 ± 0.4 (31)	10.3 ± 0.6 (24)	8.3 ± 0.3† (31)	9.8 ± 0.5 (24)
APD_{90}	20.9 ± 1.0 (30)	23.4 ± 1.5 (22)	19.9 ± 0.9 (30)	22.2 ± 1.4 (22)	18.4 ± 0.8 (30)	21.6 ± 1.3 (22)	17.6 ± 0.9 (31)	20.3 ± 1.1 (24)	16.5 ± 0.8 (31)	19.2 ± 1.0 (24)	15.7 ± 0.8† (31)	17.9 ± 0.9 (24)
LA optical APD, ms												
APD_{30}	6.1 ± 0.3 (10)	7.3 ± 0.6 (6)	6.4 ± 0.8 (10)	5.9 ± 1.0 (6)	6.1 ± 0.4 (10)	6.9 ± 1.3 (6)	4.9 ± 0.4 (10)	7.7 ± 0.9 (8)	4.6 ± 0.3 (10)	5.4 ± 0.7 (8)	4.3 ± 0.4† (10)	5.7 ± 0.7 (8)
APD_{50}	8.5 ± 0.6 (10)	10.7 ± 1.2 (6)	8.9 ± 1.1 (10)	8.5 ± 1.2 (6)	8.3 ± 0.7 (10)	10.3 ± 1.8 (6)	6.9 ± 0.4 (10)	10.0 ± 1.0 (8)	6.6 ± 0.4 (10)	8.1 ± 0.9 (8)	6.1 ± 0.4† (10)	8.0 ± 0.9 (8)
APD_{70}	11.7 ± 1.2 (10)	15.0 ± 2.1 (6)	12.5 ± 1.5 (10)	12.8 ± 1.7 (6)	11.5 ± 1.1 (10)	14.4 ± 2.5 (6)	9.4 ± 0.0 (10)	13.3 ± 1.2 (8)	9.4 ± 0.6 (10)	11.6 ± 1.5 (8)	9.1 ± 0.5† (10)	11.2 ± 1.2 (8)

Values are mean ± SEM (number of atria). *$p < 0.05$ vs. baseline. †$p < 0.05$ vs. wild-type.

APD = action potential duration; CL = cycle length; ERP = effective refractory period; *Pitx2c*$^{+/-}$ = *PITX2* deficient; other abbreviations as in Tables 1 and 2.

TABLE 4 Electrophysiological Effects of Sotalol

Paced CL, ms	Wild-Type				*Pitx2c*$^{+/-}$			
	120		100		120		100	
	Baseline	Sotalol	Baseline	Sotalol	Baseline	Sotalol	Baseline	Sotalol
LA ERP, ms								
	38.7 ± 7.8 (7)	33.9 ± 6.3 (7)	32.2 ± 6.1 (6)	29.2 ± 5.3 (6)	39.3 ± 4.0 (4)	26.8 ± 3.5 (4)	37.0 ± 5.7 (4)	24.0 ± 3.7 (4)
LA APD, ms								
APD_{50}	11.5 ± 1.2 (9)	13.4 ± 1.2 (9)	10.9 ± 2.0 (7)	12.2 ± 1.3 (7)	10.8 ± 1.1 (7)	11.2 ± 1.0 (7)	8.3 ± 0.9 (4)	11.1 ± 1.7 (4)
APD_{70}	17.6 ± 2.2 (9)	20.0 ± 1.9 (9)	16.0 ± 1.3 (7)	18.2 ± 2.3 (7)	16.5 ± 1.6 (7)	17.3 ± 1.2 (7)	13.0 ± 1.5 (4)	17.0 ± 1.9 (4)
APD_{90}	30.7 ± 3.2 (9)	33.5 ± 2.7 (9)	29.0 ± 1.9 (7)	30.9 ± 3.2 (7)	29.7 ± 2.7 (7)	31.2 ± 2.0 (7)	23.8 ± 2.8 (4)	29.6 ± 2.9 (4)

Values are mean ± SEM (number of atria).

Abbreviations as in Tables 2 and 3.

FIGURE 2 Resting Membrane Potential and Maximum Upstroke Velocity

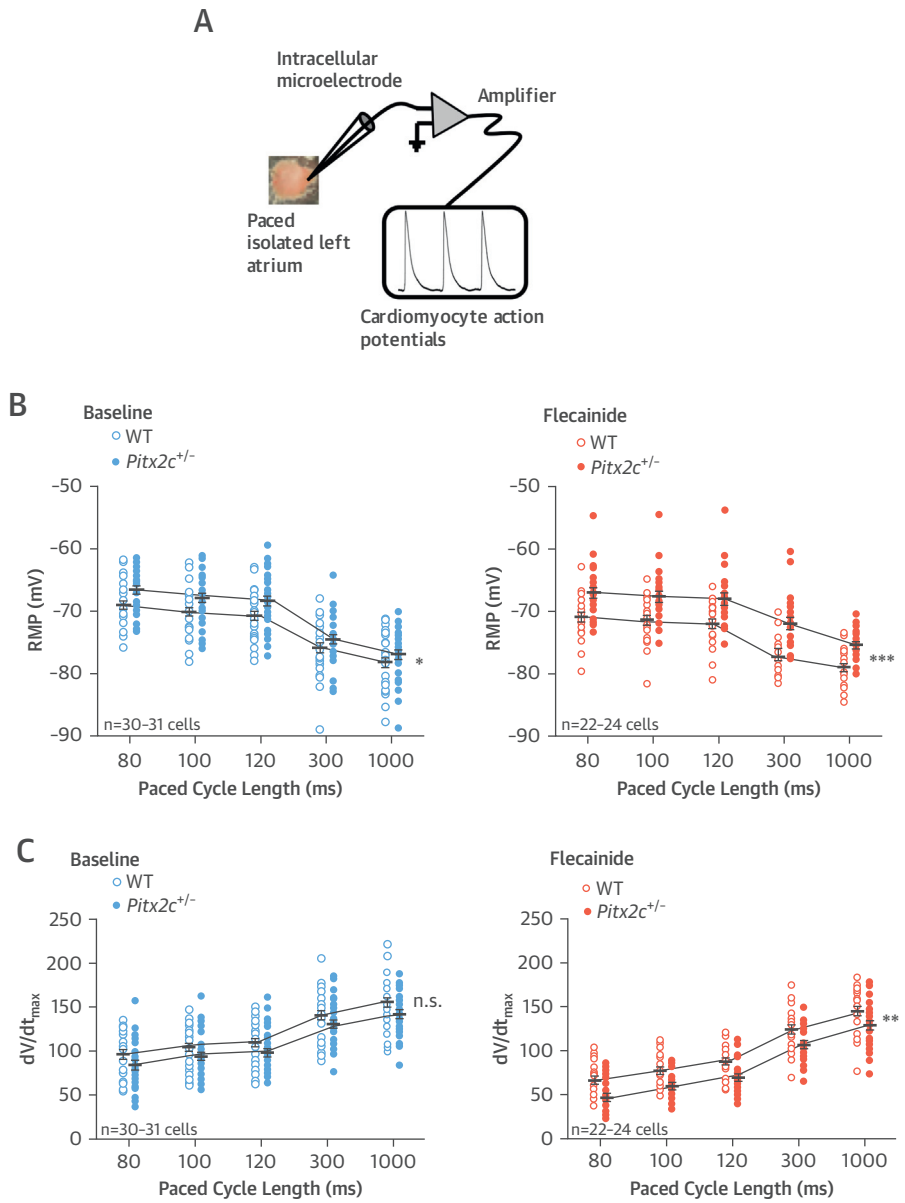

(A) Schematic representation of sharp microelectrode electrode recordings from the superfused whole LA. **(B)** Resting membrane potential (RMP) in WT and *Pitx2c*$^{+/-}$ LA at baseline and with 1 μmol/l flecainide. *Pitx2c*$^{+/-}$ LA have depolarized RMP. The difference between WT and *Pitx2c*$^{+/-}$ is exaggerated with flecainide. *p $<$ 0.05; ***p $<$ 0.001 across all cycle lengths. **(C)** Flecainide unmasked a lower maximum upstroke velocity (dV/dt_{max}) in *Pitx2c*$^{+/-}$ LA compared to WT. **p $<$ 0.01 versus WT. Abbreviations as in Figure 1.

Flecainide prolonged ERPs and refractoriness beyond the end of repolarization (PRR) calculated as the difference between ERP and APD_{90} (ms). Flecainide prolonged PRR more in hearts with reduced *Pitx2c* expression (Figures 1D and 1E, Table 3). *PITX2c*$^{+/-}$ hearts had shorter atrial action potentials (8). Flecainide abolished APD differences between *Pitx2c*$^{+/-}$ and wild-type LA by prolonging early repolarization (APD_{30}, APD_{50}, and APD_{70}) (Table 3). Murine atrial *PITX2* expression did not modulate the effects of sotalol on atrial APD or ERP (Table 4).

FIGURE 3 Modeling of the Electrophysiological Consequences of *Pitx2c* Deficiency

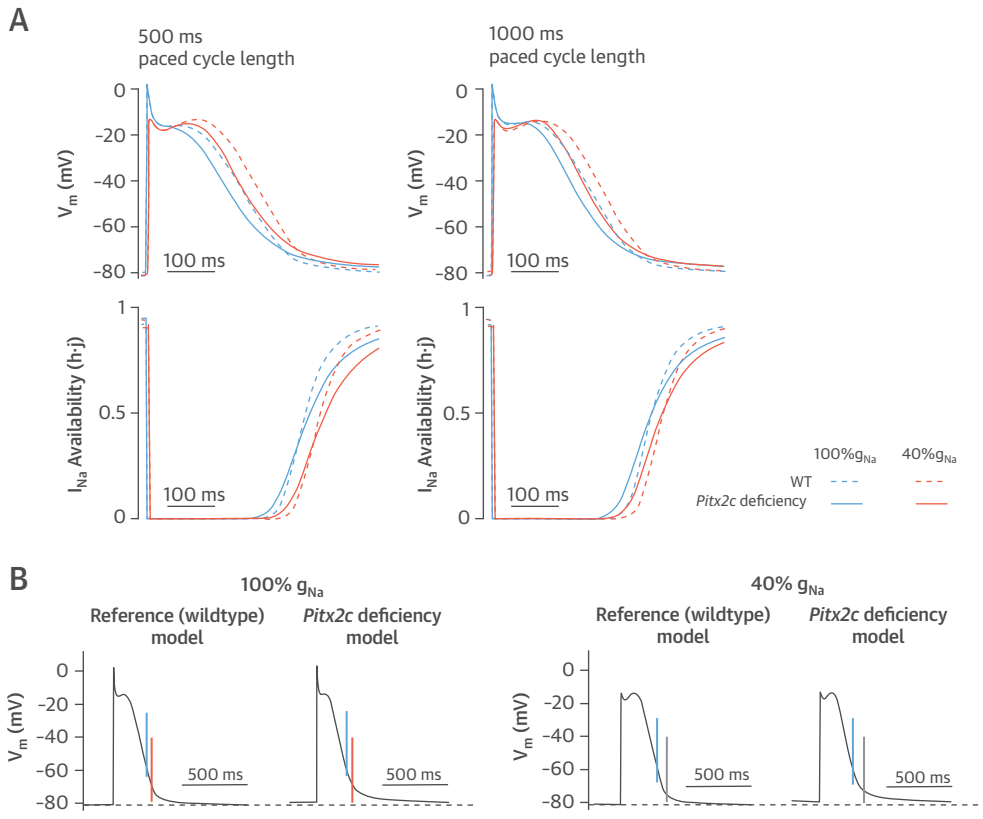

(A) Propagated action potentials **(top)** simulated with the Courtemanche-Ramirez-Nattel model modified to reflect the more positive RMP of murine *Pitx2c*$^{+/-}$ atria and the effect of 60% sodium current (I_{Na}) block at pacing cycle lengths of 500 and 1,000 ms, with 2-min pre-pacing, and corresponding time courses of the product of the 2 inactivation gates *h* and *j* of I_{Na} **(bottom),** reflecting I_{Na} availability. **(B)** Reduced sodium conductance (g_{Na}) increased post-repolarization refractoriness (PRR) in the reference model and the *Pitx2c* deficiency model. After reducing g_{Na}, PRR was greater in the *Pitx2c* deficiency model than in the reference model **(grey lines)**. Lines denote APD_{60} **(blue)** and ERP (**orange**: with 100% gNa; **grey**: with 40% gNa). Abbreviations as in Figures 1 and 2.

RMP was slightly depolarized in LA murine cells with reduced *Pitx2c* expression (range of mean depolarization 1.2 to 2.4 mV over 5 cycle lengths; all $p < 0.05$) (Figures 2A and 2B). Atrial *Pitx2c* levels did not significantly affect dV/dt_{max} (100-ms paced cycle length: wild-type: 104.4 ± 4.3 V/s; *Pitx2c*$^{+/-}$: 93.7 ± 4.5 V/s) (Figure 2C). Flecainide did not modify atrial RMP (Figure 2B) but reduced action potential amplitude consistent with its Na-channel blocking effect, specifically at 100-ms cycle length: wild-type baseline: 77.5 ± 1.2 mV (n = 30); wild-type flecainide: 71.3 ± 1.2 mV (n = 31); *Pitx2c*$^{+/-}$ baseline: 73.4 ± 1.3 mV (n = 22); and *Pitx2c*$^{+/-}$ flecainide: 65.1 ± 1.45 mV (n = 24).

Because the Courtemanche-Ramirez-Nattel model does not incorporate background K^+ currents (19), we simulated a depolarized RMP in this model by a 25% reduction in I_{K1}. This reduced the RMP at 500-ms paced cycle length by 2 mV from 79.9 mV ("normal *PITX2*") to -77.9 mV ("low *PITX2*"). Na channels recovered from inactivation more slowly upon partial I_{Na} block (50% or 60%) (Figure 3A). Furthermore, PRR was enhanced in the *PITX2* deficiency model (Figure 3B and Table 5). Inhibition of I_{Na} reduced upstroke velocity (dV/dt_{max}) and conduction velocity in both models, and reproduced the prolongation of PRR (Figure 3B).

Kcna6 and *Kcnk5* mRNA expression were reduced in *Pitx2c*$^{+/-}$ murine LA (Figure 4A, Online Table 1), whereas mRNA concentrations of 20 other ion channels or related genes were not altered. Kv1.6 protein concentration was unaltered, whereas TASK-2 protein concentration was reduced in murine atria with reduced *Pitx2c* expression (Figure 4B). $Na_v1.5$ mRNA

TABLE 5 Electrophysiological Effects of Reduced Sodium Conductance in a Human Atrial Model

	Wild-Type Model		*Pitx2c* Deficiency Model	
Paced CL, ms	**500**	**1,000**	**500**	**1,000**
RMP, mV				
g_{Na}, %				
100	-79.92	-81.28	-77.90	-79.61
50	-79.60	-81.12	-77.33	-79.37
40	-79.43	-81.01	-76.99	-79.23
APD at repolarization to -60 mV, ms				
g_{Na}, %				
100	217	253	206	226
50	239	266	233	239
40	248	273	245	245
ERP, ms				
g_{Na}, %				
100	266	301	261	280
50	308	335	316	320
40	327	352	342	339
PRR, ms				
g_{Na}, %				
100	49	48	55	54
50	69	69	83	81
40	79	79	97	94
Conduction velocity, cm/s				
g_{Na}, %				
100	49.5	50.0	50.3	50.5
50	36.9	37.0	37.5	37.5
40	32.9	32.7	33.0	33.1

g_{Na} = reduced sodium conductance; PRR = post-repolarization refractoriness; RMP = resting membrane potential; other abbreviations as in Table 3.

and protein expression were not changed (**Figures 4A and 4B**).

Atrial *Pitx2c* expression did not modify peak Na^+ currents (I_{Na}) recorded from isolated murine cardiomyocytes at holding potentials ranging from -100 to -65 mV (**Figures 5A to 5C**). Peak I_{Na} was reduced at more depolarized holding potentials (**Figure 5**). Flecainide inhibited I_{Na} better at more positive holding potentials (inhibition at -70 mV: 68 ± 5%; inhibition at -65 mV: 75 ± 5%; n = 86 cells from n = 17 atria) in cells from murine atria with normal or reduced *Pitx2c* expression, suggesting that the greater efficiency of flecainide in atria with reduced *Pitx2c* expression is secondary to RMP depolarization (**Figure 5C**). Consistent with this, flecainide inhibited human $Na_v1.5$ channels expressed in HEK cells more potently at more depolarized test potentials (-65 to -75 mV) (**Figures 5D and 5E**).

Background K^+ currents, which include TASK currents, were reduced in *Pitx2c*$^{+/-}$ murine atria, whereas I_{K1} did not differ between genotypes (**Figure 6**).

Reduced *Pitx2c* expression did not alter atrial conduction velocities or activation patterns (Online Figures 1A to 1C, **Table 6**), consistent with published data (8). We found that 1 μmol/l flecainide decreased atrial conduction velocities without differences between wild-type and *Pitx2c*$^{+/-}$ mice (Online Figures 1B and 1C). Calcium transient relaxation times at 50% relaxation were not different between wild-type and *Pitx2c*$^{+/-}$ (Online Figures 1D and 1E). Flecainide 1 μmol/l shortened 50% Ca^{2+} relaxation times by approximately 10% and decreased Ca^{2+} transient amplitude by approximately 50% in murine atria with normal and reduced *Pitx2c* expression (Online Figures 1E and 1F). Additionally, expression of the Na/Ca exchanger Serca2a and Na/K ATPase alpha-1 and alpha-2 subunit protein did not differ between wild-type and *Pitx2c*$^{+/-}$ atria (Online Figure 2).

DISCUSSION

This study demonstrated that LA *PITX2* mRNA concentrations vary in patients with AF requiring rhythm control therapy (**Central Illustration**). Furthermore, flecainide increases PRR and suppresses arrhythmias more effectively in atria with halved *Pitx2c* expression, mediated by a more depolarized RMP (**Central Illustration**). Drug-induced PRR is thought to prevent arrhythmias, as reactivation can then occur only after full recovery of excitability, avoiding slow propagation during the vulnerable period (16,24,25). We found similar effects in cells expressing human Na channels and in the Courtemanche-Ramirez-Nattel model of human atrial action potentials.

Thus, this study highlighted modulation of the atrial RMP by *PITX2*, possibly mediated by background currents such as TASK-2, as a target for AAD therapy, including atrial-selective therapy. Furthermore, the results suggested that markers for atrial *PITX2* expression may identify AF patients who benefit from Na-channel blocker therapy (**Central Illustration**).

Low atrial *PITX2* expression was identified as an important determinant of the antiarrhythmic effects of Na channel blockers. Low LA *Pitx2c* mRNA depolarized atrial RMP (**Figure 2**), consistent with a previous report (11). A depolarized RMP increased flecainide-induced PRR (**Figure 1**) (26-30). The conduction-slowing effect of flecainide was not modulated by reduced atrial *Pitx2c* (Online Figure 1), an important surrogate for drug safety. Both the modeling experiments (**Figure 3**) and the experiments in HEK cells expressing human Na channels (**Figure 5**)

FIGURE 4 mRNA and Protein Expression in Murine LA

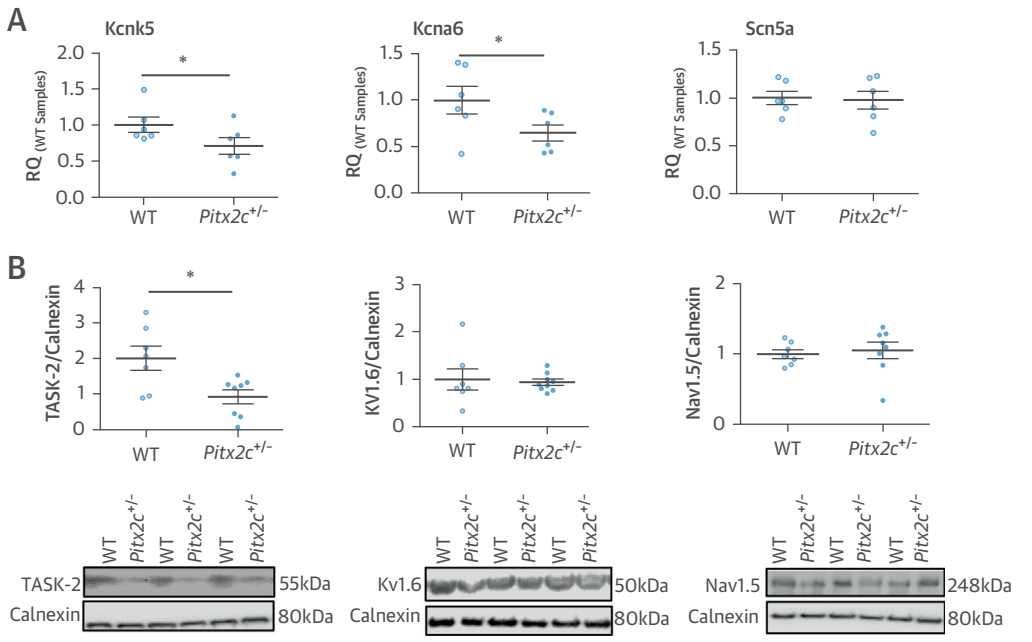

(A) Relative quantity (RQ) of messenger ribonucleic acid (mRNA) of selected ion channels in LA from *Pitx2c*$^{+/-}$ and WT mice. Expression levels were measured relative to WT sample 1. Kcnk5 encodes TWIK-related acid-sensitive K^+ channel 2 (TASK-2), Kcna6 encodes K_v1.6, and Scn5a encodes Na_v1.5. *$p < 0.05$. **(B)** Concentration of TASK-2, K_v1.6, and Na_v1.5 proteins relative to calnexin (arbitrary units). Representative immunoblots are displayed below the corresponding dot plot. *$p < 0.05$. Abbreviations as in Figures 1 and 2.

confirmed that small changes in RMP can markedly modulate Na-channel inhibition.

RESTING MEMBRANE POTENTIAL. Open-state Na-channel blockers such as flecainide and propafenone bind preferentially to Na channels integrated in membranes with slightly depolarized resting potentials, where more channels are in the open or inactivated state (31,32). Our data can be interpreted as suggesting that AAD combinations that include a Na-channel blocker with a membrane potential modifying substance, such as amiodarone (16,33) or the combination of dronedarone and ranolazine (29,34,35), may have synergistic antiarrhythmic effects because they modulate atrial RMP and thereby enhance the effect of Na-channel blockade. Further studies of such drug combinations and the relationship between their effectiveness and the patient's atrial *PITX2* mRNA levels are warranted. Our data also suggested that such combined effects may be of special relevance in patients who have a depolarized RMP, such as secondary to low LA *PITX2*. Because *PITX2* expression is confined to the LA in the heart, AAD therapy that leverages modifications in RMP may achieve "atrial-specific" AAD therapy.

RMP is maintained by an intricate balance of different transmembrane currents and is closely related to the potassium equilibrium potential. We identified that *PITX2* modifies expression of the genes encoding K_v1.6 and TASK-2 (Figure 4). Complete deletion of *PITX2* regulates other potassium and Na channels such as *Kcnj2* (8,36), which alter the RMP, but these were not responsible for the depolarized RMP observed in our study. Two-pore domain potassium channels, such as TASK-2, contribute to RMP in various cells, including skeletal and cardiac muscle (37,38). To date, an altered function of the TASK-1 channel and of I_{K1} has been implicated in atrial remodeling and AF (39,40). This study demonstrated that TASK-2 is expressed in atrial myocardium (Figure 4B), suggesting that a reduced function of TASK-2 could depolarize RMP (Figures 1 and 5) (8,11), analogous to the effect of TASK-2 in neuronal and cartilage tissue (41,42).

DEVELOPING CLINICAL MARKERS FOR PATIENTS WITH DEPOLARIZED RMP. It will be challenging to directly assess LA RMP in AF patients, but our data suggested that differences in atrial RMP could explain the effectiveness of Na-channel blockers in carriers of

FIGURE 5 Effect of Membrane Potential on Sodium-Channel Inhibition

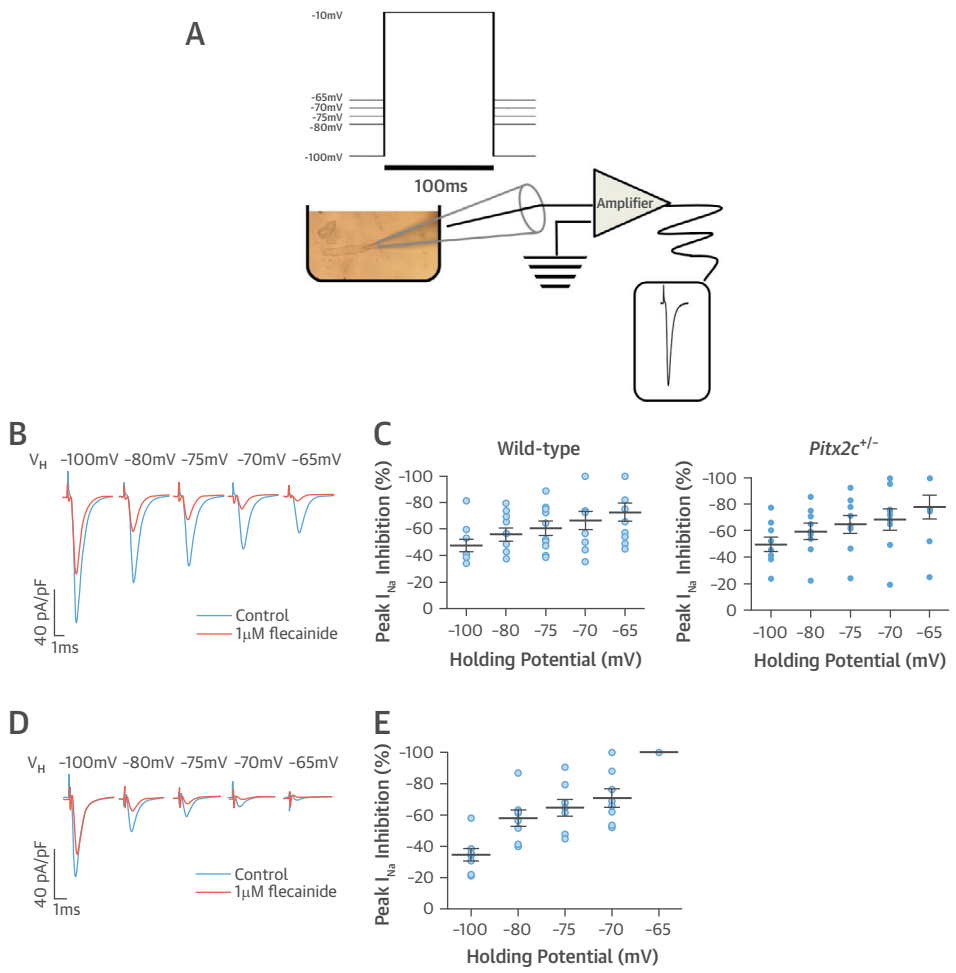

(A) Schematic representation of patch clamp experiments carried out in isolated atrial cardiomyocytes. Human embryonic kidney (HEK) cells were patch clamped using the same setup. **(B)** Representative traces showing I_{Na} measured by patch clamping in isolated atrial cardiomyocytes, at baseline and with flecainide, at increasing holding potentials (-100 to -65 mV). **(C)** Reduction in peak I_{Na} was enhanced with increased holding potentials, irrespective of cardiomyocyte origin. **(D)** Representative traces showing I_{Na} in $Na_v1.5$-transfected HEK cells at baseline and with flecainide at increasing holding potentials (-100 to -65 mV). **(E)** Reduction in peak I_{Na} with flecainide in $Na_v1.5$-transfected HEK cells was enhanced with increased holding potentials. The greatest difference in percent reduction was between -70 and -65 mV. Abbreviations as in Figures 1 to 3.

common gene variants on chromosome 4q25 (43), although LA *PITX2* levels are modulated by factors other than SNP status (Table 2) (44). It seems desirable to develop and validate drivers that modify RMP and clinical markers for patients prone to a depolarized atrial RMP to select appropriate AADs for individual patients in the future, thus enabling personalized AAD selection (6,45).

STUDY LIMITATIONS. This study provided robust evidence that LA *PITX2* expression varies in AF patients and that reduced *PITX2c* expression enhances the antiarrhythmic effects of Na-channel blockers by modulating atrial RMP. The study was partly motivated by the assumption that gene variants on chromosome 4q25 modify *PITX2* expression, an assumption that has not been definitively proven (9,11,44,46). Our analysis (Table 2) and that of others indicate that SNP status does not always correlate with *PITX2* levels (47,48). Our findings are relevant to AAD therapy even if the presumed link between *PITX2* expression and genetic variants on

FIGURE 6 Currents Responsible for RMP

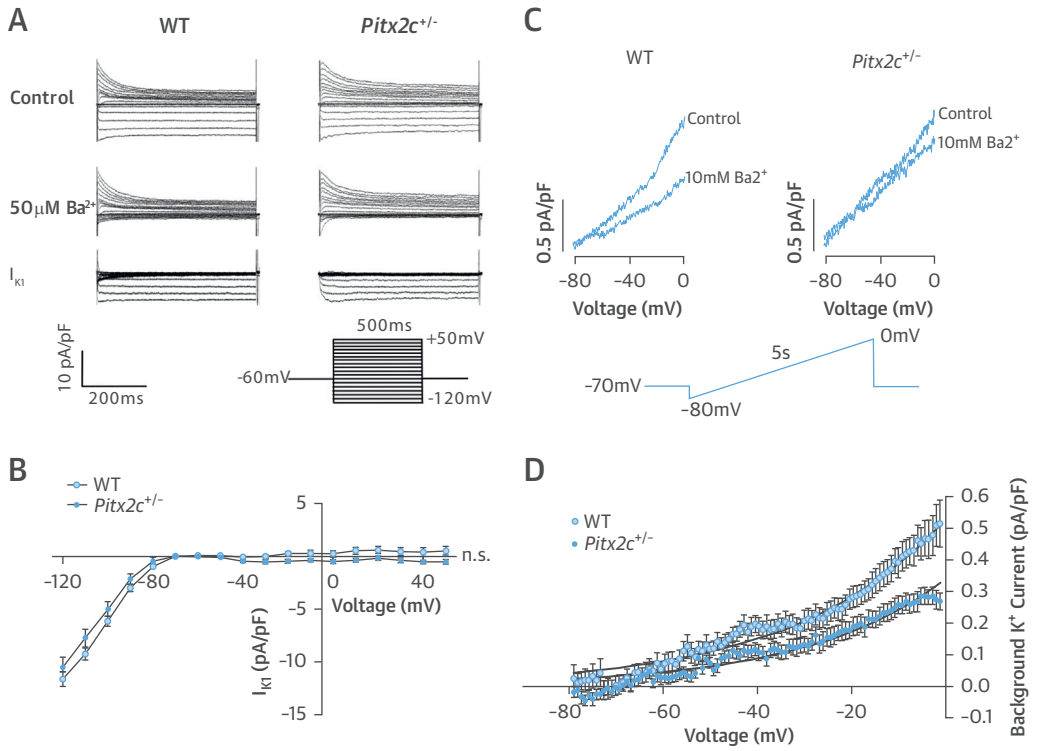

(A) Representative raw traces showing I_{K1} currents (50 μmol/l Ba^{2+} sensitive) in isolated WT and *Pitx2c*$^{+/-}$ LA cardiomyocytes at test potentials ranging from –120 to 50mV. **(B)** No difference is seen in the I_{K1} current/voltage relationship for LA cardiomyocytes between WT and *Pitx2c*$^{+/-}$ LA at test potentials ranging from –120 to 50 mV. **(C)** Representative raw traces show background current response to 10 mmol/l Ba^{2+} in isolated WT and *Pitx2c*$^{+/-}$ LA cardiomyocytes. **(D)** *Pitx2c*$^{+/-}$ cardiomyocytes had significantly reduced background K^+ (10 mmol/l Ba^{2+} sensitive) currents than WT cardiomyocytes. *$p < 0.05$. Abbreviations as in Figures 1 to 3.

chromosome 4q25 proves elusive. The mechanisms by which reduced *PITX2* mRNA concentrations shorten the LA action potential at high heart rates remain to be fully elucidated (8,20). Validating our findings in patients is desirable but will be challenging because access to fresh LA cardiomyocytes and LA tissue is limited.

Due to the novelty of our findings, we could not perform a priori power calculations for our mechanistic experiments, and we analyzed several functional parameters to identify potential mechanisms conveying the antiarrhythmic effects of flecainide in atria with low *Pitx2c* concentrations. Our findings thus require independent validation.

TABLE 6 Electrical Activation Time and Conduction Velocity in Isolated Atria in the Presence of Flecainide (1 μmol/l)

	Wild-Type					*Pitx2c*$^{+/-}$				
Paced CL, ms	1,000	300	120	100	80	1,000	300	120	100	80
Activation time (isolated left atrium), ms	6 ± 0.3 (22)	6 ± 0.3 (22)	9 ± 0.5 (22)	12 ± 1.0 (22)	16 ± 1.4 (22)	6 ± 0.2 (24)	7 ± 0.3 (24)	12 ± 0.9 (24)	13 ± 0.9 (24)	18 ± 1.2 (24)
Conduction velocity (optical mapping), cm/s	–	30 ± 1.8 (8)	25 ± 2.4 (8)	25 ± 1.9 (8)	23 ± 1.9 (8)	–	29 ± 1.5 (8)	26 ± 1.6 (8)	25 ± 1.6 (8)	23 ± 1.6 (8)

Values are mean ± SEM (number of atria).
– = not applicable; other abbreviations as in Table 3.

CENTRAL ILLUSTRATION ***PITX2* Deficiency Potentiates Flecainide's Antiarrhythmic Effects**

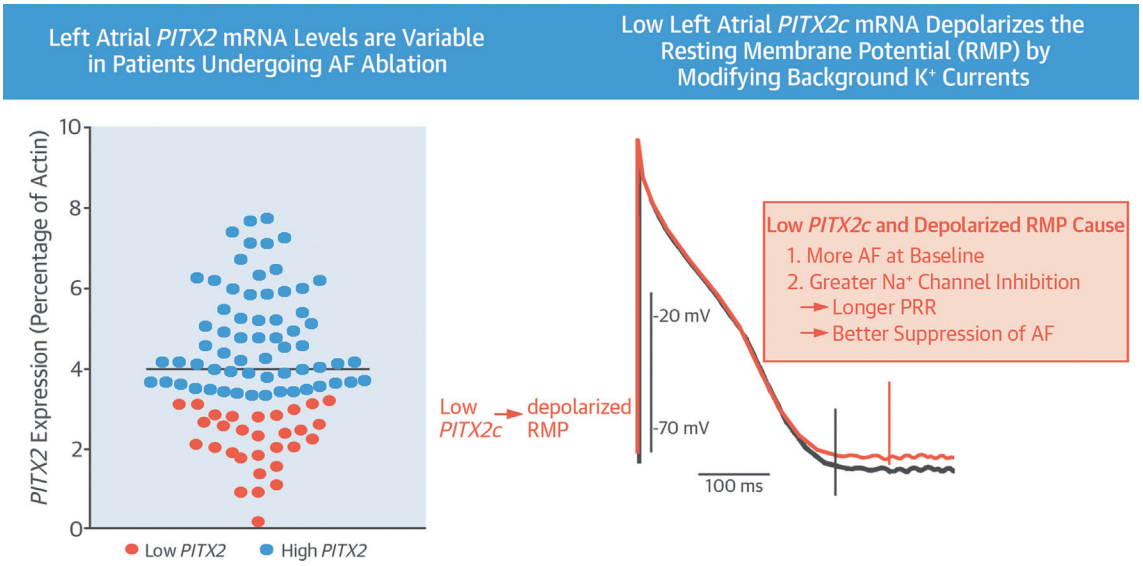

Syeda, F. et al. J Am Coll Cardiol. 2016;68(17):1881–94.

Paired like homeodomain 2 (*PITX2*) might play an important role in regulating gene expression and electrical function of the left atrium. **(Left)** *Pitx2* messenger ribonucleic acid (mRNA) levels are variable in left atrial appendages of patients undergoing thoracoscopic atrial fibrillation (AF) ablation therapy. The differentiation between "low" **(orange)** and "high" **(blue)** *PITX2* levels is somewhat arbitrary. **(Right)** A low left atrial *PITX2c* mRNA expression slightly depolarizes left atrial resting membrane potential (RMP). A depolarized RMP, in turn, enhances the antiarrhythmic effect of sodium-channel blockers such as flecainide. PRR = post-repolarization refractoriness.

CONCLUSIONS

This study shows that low LA *PITX2* mRNA levels increase atrial RMP and thereby increase the effectiveness of flecainide (Central Illustration). This finding calls for appropriately designed clinical studies to assess whether AF patients with low atrial *PITX2* levels respond favorably to Na-channel blockade. Further studies exploring the relevance of TASK channels to atrial RMP also are warranted.

ACKNOWLEDGMENTS The authors thank Sian Marie O'Brien, Sarah Hopkins, Syeeda Nashitha Kabir, Pushpa Patel, and Charles Carey for technical support; Marta Coric for help with HEK cells; and Ilaria Piccini for advice on TLDA.

REPRINT REQUESTS AND CORRESPONDENCE: Prof. Paulus Kirchhof, Institute of Cardiovascular Sciences, University of Birmingham, Wolfson Drive, Birmingham B15 2TT, United Kingdom. E-mail: p.kirchhof@bham.ac.uk.

PERSPECTIVES

COMPETENCY IN MEDICAL KNOWLEDGE: *PITX2*, a transcription factor linked to left-right asymmetry in the chest during development, modulates the expression of LA ion channels maintaining the RMP and modulates the antiarrhythmic effects of Na-channel blockers.

TRANSLATIONAL OUTLOOK: Clinical studies are needed to assess whether reduced *PITX2* expression identifies patients with AF who respond favorably to Na-channel blocking drugs.

REFERENCES

1. Chugh SS, Havmoeller R, Narayanan K, et al. Worldwide epidemiology of atrial fibrillation: a Global Burden of Disease 2010 Study. Circulation 2014;129:837–47.

2. January CT, Wann LS, Alpert JS, et al. 2014 AHA/ACC/HRS guideline for the management of

patients with atrial fibrillation: a report of the American College of Cardiology/American Heart Association Task Force on Practice Guidelines and the Heart Rhythm Society. J Am Coll Cardiol 2014; 64:e1–76.

3. Kirchhof P, Benussi S, Kotecha D, et al. 2016 ESC Guidelines for the management of atrial fibrillation developed in collaboration with EACTS: The Task Force for the management of atrial fibrillation of the European Society of Cardiology (ESC) developed with the special contribution of the European Heart Rhythm Association (EHRA) of the ESC Endorsed by the European Stroke Organisation (ESO). Eur Heart J 2016 Aug 27 [E-pub ahead of print].

4. Kirchhof P, Andresen D, Bosch R, et al. Short-term versus long-term antiarrhythmic drug treatment after cardioversion of atrial fibrillation (Flec-SL): a prospective, randomised, open-label, blinded endpoint assessment trial. Lancet 2012; 380:238–46.

5. Schotten U, Verheule S, Kirchhof P, Goette A. Pathophysiological mechanisms of atrial fibrillation: a translational appraisal. Physiol Rev 2011;91: 265–325.

6. Fabritz L, Guasch E, Antoniades C, et al. Expert consensus document: defining the major health modifiers causing atrial fibrillation: a roadmap to underpin personalized prevention and treatment. Nat Rev Cardiol 2015;13:230–7.

7. Li N, Dobrev D, Wehrens XH. PITX2: a master regulator of cardiac channelopathy in atrial fibrillation? Cardiovasc Res 2016;109:345–7.

8. Kirchhof P, Kahr PC, Kaese S, et al. PITX2c is expressed in the adult left atrium, and reducing Pitx2c expression promotes atrial fibrillation inducibility and complex changes in gene expression. Circ Cardiovasc Genet 2011;4: 123–33.

9. Kahr PC, Piccini I, Fabritz L, et al. Systematic analysis of gene expression differences between left and right atria in different mouse strains and in human atrial tissue. PLoS One 2011;6:e26389.

10. Wang J, Klysik E, Sood S, et al. Pitx2 prevents susceptibility to atrial arrhythmias by inhibiting left-sided pacemaker specification. Proc Natl Acad Sci U S A 2010;107:9753–8.

11. Chinchilla A, Daimi H, Lozano-Velasco E, et al. PITX2 insufficiency leads to atrial electrical and structural remodeling linked to arrhythmogenesis. Circ Cardiovasc Genet 2011;4:269–79.

12. Driessen AH, Berger WR, Krul SP, et al. Ganglion plexus ablation in advanced atrial fibrillation. The (AFACT) study. J Am Coll Cardiol 2016;68: 1155–65.

13. Krul SP, Driessen AH, van Boven WJ, et al. Thoracoscopic video-assisted pulmonary vein antrum isolation, ganglionated plexus ablation, and periprocedural confirmation of ablation lesions: first results of a hybrid surgical-electrophysiological approach for atrial fibrillation. Circ Arrhythm Electrophysiol 2011;4:262–70.

14. Lubitz SA, Lunetta KL, Lin H, et al. Novel genetic markers associate with atrial fibrillation risk in Europeans and Japanese. J Am Coll Cardiol 2014;63:1200–10.

15. Blana A, Kaese S, Fortmuller L, et al. Knock-in gain-of-function sodium channel mutation prolongs atrial action potentials and alters atrial vulnerability. Heart Rhythm 2010;7:1862–9.

16. Kirchhof P, Degen H, Franz MR, et al. Amiodarone-induced postrepolarization refractoriness suppresses induction of ventricular fibrillation. J Pharmacol Exp Ther 2003;305:257–63.

17. Yu TY, Syeda F, Holmes AP, et al. An automated system using spatial oversampling for optical mapping in murine atria. Development and validation with monophasic and transmembrane action potentials. Prog Biophys Mol Biol 2014;115: 340–8.

18. Lemoine MD, Duverger JE, Naud P, et al. Arrhythmogenic left atrial cellular electrophysiology in a murine genetic long QT syndrome model. Cardiovasc Res 2011;92:67–74.

19. Courtemanche M, Ramirez RJ, Nattel S. Ionic mechanisms underlying human atrial action potential properties: insights from a mathematical model. Am J Physiol 1998;275:H301–21.

20. Holmes AP, Yu TY, Tull S, et al. A regional reduction in Ito and IKACh in the murine posterior left atrial myocardium is associated with action potential prolongation and increased ectopic activity. PLoS One 2016;11:e0154077.

21. Barbuti A, Ishii S, Shimizu T, Robinson RB, Feinmark SJ. Block of the background K(+) channel TASK-1 contributes to arrhythmogenic effects of platelet-activating factor. Am J Physiol Heart Circ Physiol 2002;282:H2024–30.

22. Buckler KJ. A novel oxygen-sensitive potassium current in rat carotid body type I cells. J Physiol 1997;498 Pt 3:649–62.

23. Limberg SH, Netter MF, Rolfes C, et al. TASK-1 channels may modulate action potential duration of human atrial cardiomyocytes. Cell Physiol Biochem 2011;28:613–24.

24. Kirchhof P, Fabritz L, Franz MR. Post-repolarization refractoriness versus conduction slowing caused by class I antiarrhythmic drugs: antiarrhythmic and proarrhythmic effects. Circulation 1998;97:2567–74.

25. Milberg P, Frommeyer G, Uphaus T, et al. Electrophysiologic profile of dronedarone on the ventricular level: beneficial effect on post-repolarization refractoriness in the presence of rapid phase 3 repolarization. J Cardiovasc Pharmacol 2012;59:92–100.

26. Frommeyer G, Schmidt M, Clauss C, et al. Further insights into the underlying electrophysiological mechanisms for reduction of atrial fibrillation by ranolazine in an experimental model of chronic heart failure. Eur J Heart Fail 2012;14: 1322–31.

27. Milberg P, Frommeyer G, Ghezelbash S, et al. Sodium channel block by ranolazine in an experimental model of stretch-related atrial fibrillation: prolongation of interatrial conduction time and increase in post-repolarization refractoriness. Europace 2013;15:761–9.

28. Fukuda K, Watanabe J, Yagi T, et al. A sodium channel blocker, pilsicainide, produces atrial post-repolarization refractoriness through the reduction of sodium channel availability. Tohoku J Exp Med 2011;225:35–42.

29. Burashnikov A, Sicouri S, Di Diego JM, Belardinelli L, Antzelevitch C. Synergistic effect of the combination of ranolazine and dronedarone to suppress atrial fibrillation. J Am Coll Cardiol 2010; 56:1216–24.

30. Kirchhof P, Engelen M, Franz MR, et al. Electrophysiological effects of flecainide and sotalol in the human atrium during persistent atrial fibrillation. Basic Res Cardiol 2005;100:112–21.

31. Anno T, Hondeghem LM. Interactions of flecainide with guinea pig cardiac sodium channels. Importance of activation unblocking to the voltage dependence of recovery. Circ Res 1990; 66:789–803.

32. Nitta J, Sunami A, Marumo F, Hiraoka M. States and sites of actions of flecainide on guinea-pig cardiac sodium channels. Eur J Pharmacol 1992; 214:191–7.

33. Singh BN, Singh SN, Reda DJ, et al. Amiodarone versus sotalol for atrial fibrillation. N Engl J Med 2005;352:1861–72.

34. Burashnikov A, Di Diego JM, Zygmunt AC, et al. Atrial-selective sodium channel block as a strategy for suppression of atrial fibrillation. Ann N Y Acad Sci 2008;1123:105–12.

35. Reiffel JA, Camm AJ, Belardinelli L, et al. The HARMONY trial: combined ranolazine and dronedarone in the management of paroxysmal atrial fibrillation: mechanistic and therapeutic synergism. Circ Arrhythm Electrophysiol 2015;8: 1048–56.

36. Tao Y, Zhang M, Li L, et al. Pitx2, an atrial fibrillation predisposition gene directly regulates ion transport and intercalated disc genes. Circ Cardiovasc Genet 2014;7:23–32.

37. Reyes R, Duprat F, Lesage F, et al. Cloning and expression of a novel pH-sensitive two pore domain K+ channel from human kidney. J Biol Chem 1998;273:30863–9.

38. Enyedi P, Czirjak G. Molecular background of leak K+ currents: two-pore domain potassium channels. Physiol Rev 2010;90:559–605.

39. Harleton E, Besana A, Chandra P, et al. TASK-1 current is inhibited by phosphorylation during human and canine chronic atrial fibrillation. Am J Physiol Heart Circ Physiol 2015;308: H126–34.

40. Liang B, Soka M, Christensen AH, et al. Genetic variation in the two-pore domain potassium channel, TASK-1, may contribute to an atrial substrate for arrhythmogenesis. J Mol Cell Cardiol 2014;67:69–76.

41. Clark RB, Kondo C, Belke DD, Giles WR. Two-pore domain K(+) channels regulate membrane potential of isolated human articular chondrocytes. J Physiol 2011;589:5071–89.

42. Kindler CH, Paul M, Zou H, et al. Amide local anesthetics potently inhibit the human tandem pore domain background K+ channel TASK-2 (KCNK5). J Pharmacol Exp Ther 2003;306: 84–92.

43. Ellinor PT, Lunetta KL, Albert CM, et al. Meta-analysis identifies six new susceptibility

loci for atrial fibrillation. Nat Genet 2012;44:670–5.

44. Gore-Panter SR, Hsu J, Barnard J, et al. PANCR, the PITX2 Adjacent noncoding RNA, is expressed in human left atria and regulates PITX2c expression. Circ Arrhythm Electrophysiol 2016;9:e003197.

45. Kirchhof P, Sipido KR, Cowie MR, et al. The continuum of personalized cardiovascular medicine: a position paper of the European Society of Cardiology. Eur Heart J 2014;35:3250–7.

46. Holmes AP, Kirchhof P. Pitx2 adjacent non-coding RNA: a new, long, noncoding kid on the 4q25 Block. Circ Arrhythm Electrophysiol 2016;9:e003808.

47. Martin RI, Babaei MS, Choy MK, et al. Genetic variants associated with risk of atrial fibrillation regulate expression of PITX2, CAV1, MYOZ1, C9orf3 and FANCC. J Mol Cell Cardiol 2015;85:207–14.

48. Gore-Panter SR, Hsu J, Hanna P, et al. Atrial fibrillation associated chromosome 4q25 variants are not associated with PITX2c expression in human adult left atrial appendages. PLoS One 2014;9:e86245.

KEY WORDS antiarrhythmic drugs, atrial fibrillation, drug targets, electrophysiology, personalized medicine, rhythm control

APPENDIX For an expanded Methods section as well as supplemental figures and a table, please see the online version of this article.

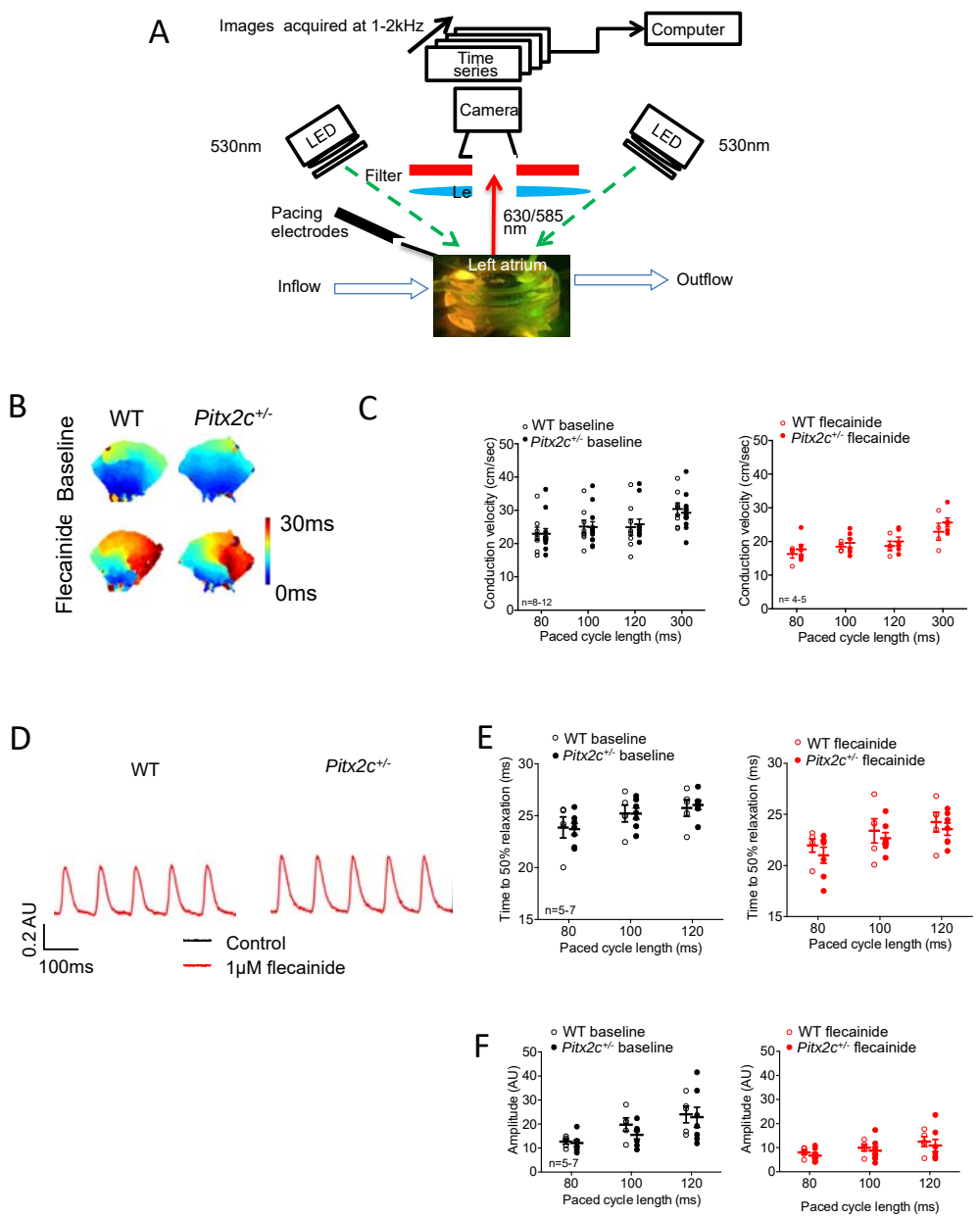

Supplementary Figure 1

Supplementary Figure 1

A Experimental setup of the high density optical activation mapping system. This system was also used to measure Ca^{2+} transients.

B Representative electrical activation maps of wildtype (WT) and *Pitx2c*$^{+/-}$ LA before and after flecainide, recorded at 100ms cycle length pacing. Flecainide causes conduction slowing in both genotypes to the same degree.

C Conduction velocity determined by optical activation mapping in superfused *Pitx2c*$^{+/-}$ and wildtype LA, measured at 80-300ms paced CL. Baseline (black): wildtype n=5; *Pitx2c*$^{+/-}$ n=11. Flecainide (red): wildtype: n=4; *Pitx2c*$^{+/-}$ n= 8. Individual values are displayed. Data points for each genotype have been offset at each cycle length for clarity.

D Representative calcium transients recorded during 100ms cycle length pacing at baseline (black) and with 1µmol/L flecainide (red) from isolated superfused wildtype and *Pitx2c*$^{+/-}$ LA . Calcium transients did not differ between genotypes with or without flecainide. Horizontal line= 40 ms.

E Time to 50% calcium relaxation at baseline and after 1µmol/L flecainide in LA. Calcium relaxation time did not differ between genotypes with or without flecainide. Baseline (black): wildtype n=5; *Pitx2c*$^{+/-}$ n=7. Flecainide (red): wildtype: n=5; *Pitx2c*$^{+/-}$ n= 7.

F Calcium signal amplitude at baseline and after 1 µmol/L flecainide in LA. AU= arbitrary units; fold-change in fluorescence. Baseline (black): wildtype n=5; *Pitx2c*$^{+/-}$ n=7. Flecainide (red): wildtype: n=5; *Pitx2c*$^{+/-}$ n= 7. Data points for each genotype have been offset at each cycle length for clarity.

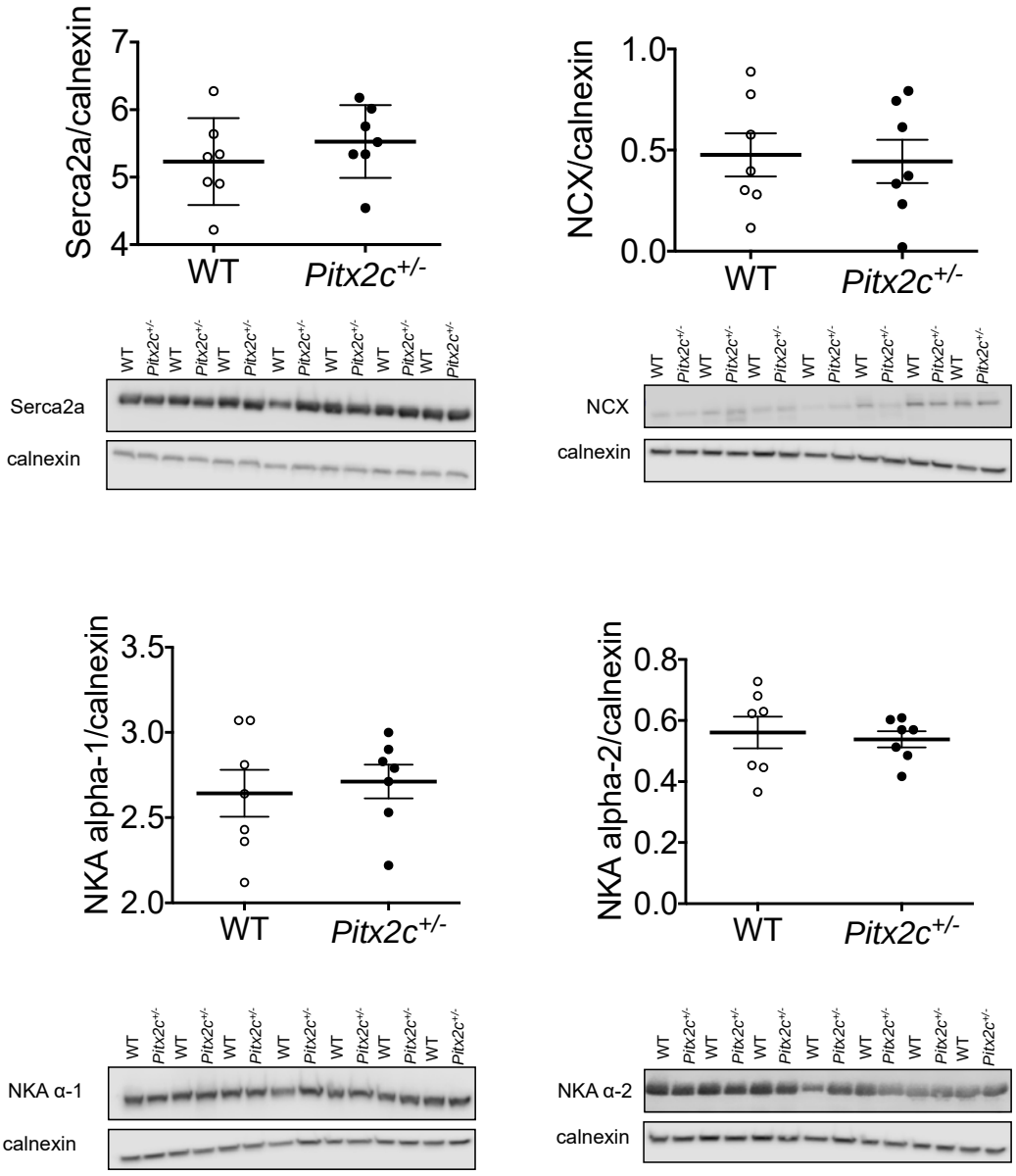

Supplementary Figure 2

Supplementary Figure 2

Protein concentrations of Na/Ca exchanger, Serca2a, Na/K ATPase alpha-1 and alpha-2 proteins, relative to calnexin (arbitrary units) in left atrial homogenates of wild type (WT) and heterozygous *Pitx2c*$^{+/-}$ mice. Representative immunoblots are displayed below the corresponding dot plot. WT = 7, *Pitx2c*$^{+/-}$ = 7.

Supplementary Table: Quantification of mRNA of ion channels in left atria from *Pitx2c*$^{+/-}$ and wild-type mice. Expression levels were measured relative to wildtype sample 1. * and boldface indicate p<0.05

Gene	Protein	WT $Rq_{control}$ ±SEM	*Pitx2c*$^{+/-}$ $Rq_{control}$ ±SEM	Mean CT ±SEM
Pitx2	PITX2	1 ± 0.13	0.77 ± 0.09	26.4* ± 0.12
Kcna6	K_v1.6	1 ± 0.15	0.65 ± 0.09	27.2* ± 0.17
Kcnk5	TASK-2	1 ± 0.1	0.71 ± 0.12	28.6* ± 0.13
Actb	ACTB	1 ± 0.19	0.84 ± 0.09	19.7 ± 0.06
Cacna1c	Cav1.2	1 ± 0.08	1.03 ± 0.08	22.7 ± 0.11
Cacna2d2	CACNA2D	1 ± 0.11	1.27 ± 0.15	25.1 ± 0.17
Casq2	CSQ2	1 ± 0.06	0.98 ± 0.06	19.9 ± 0.18
Cul7	P185	1 ± 0.07	0.96 ± 0.08	25.5 ± 0.1
Itpr2	AI649341	1 ± 0.14	0.87 ± 0.07	25.3 ± 0.11
Kcna3	K_v1.3	1 ± 0.8	0.16 ± 0.03	31.6± 0.17
Kcna4	K_v1.4	1 ± 0.12	0.94 ± 0.08	27.7 ± 0.16
Kcnc4	K_v3.4	1 ± 0.43	0.85 ± 0.39	32.3 ± 0.43
Kcnj2	IRK1	1 ± 0.07	0.91 ± 0.07	23.9 ± 0.12
Kcnj3	GIRK-1	1 ± 0.05	0.98 ± 0.03	19.5 ± 0.13
Kcnj5	GIRK4	1 ± 0.08	0.95 ± 0.07	21.5 ± 0.11
Ryr2	RYR2	1 ± 0.09	0.88 ± 0.06	18.4 ± 0.11
Scn1b	SCN1B	1 ± 0.08	0.88 ± 0.06	23.6± 0.1
Scn4a	Na_v1.4	1 ± 0.1	1.25 ± 0.12	24.4 ± 0.11
Scn5a	Na_v1.5	1 ± 0.07	0.98 ± 0.1	21.2± 0.1
Scn7a	Na_v2	1 ± 0.13	0.8 ± 0.04	24 ± 0.09
Trpc1	TRP1	1 ± 0.07	0.94 ± 0.06	26.5± 0.1
Trpc6	TRP-6	1 ± 0.13	0.88 ± 0.14	31.1 ± 0.15
Trpm7	TRPM7	1 ± 0.12	0.84 ± 0.04	23.7 ± 0.12

Supplementary methods

Electrophysiological study in the isolated heart.

Mice were terminally anaesthetized with 400mg/kg pentobarbital sodium and heparinized. Their hearts were rapidly excised, mounted on a Langendorff apparatus (Hugo Sachs, Germany) and retrogradely perfused with 37°C Krebs-Henseleit (KH) containing (in mmol/l): NaCl 118; $NaHCO_3$ 24.88; KH_2PO_4 1.18; Glucose 5.55; Na-Pyruvate 5; $MgSO_4$ 0.83; $CaCl_2$ 1.8; KCl 3.52 (95% O_2–5% CO_2, pH 7.4) at constant perfusion pressure (100 ± 5 mmHg) and coronary flow (4 ± 0.5ml/min).

A 2.0 French octapolar mouse electrophysiological catheter (0.5 mm electrode spacing, CIB'ER MOUSE, NuMED, USA) was inserted into the right atrium and right ventricle for pacing and recording intracardiac electrograms. Left atrial epicardial monophasic action potentials (MAP) were recorded using custom-made electrodes, preamplified using a DC-coupled pre amplifier (Model 2000, EP Technologies, USA), recorded at 2 kHz sampling frequency, and analyzed offline (EMKA technologies, France). Inducibility of atrial arrhythmias (triplets, salvos and AF) and effective refractory periods, with and without flecainide acetate (Sigma, 1µmol/L) and sotalol hydrochloride (Sigma, 10µmol/L), were determined using 120 to 80 ms paced cycle lengths and premature single RA extrastimulus. Activation times and action potential durations at different repolarization levels were analyzed.

Transmembrane action potential recordings in isolated, superfused left atria.

Transmembrane action potentials were recorded using borosilicate glass microelectrodes, filled with 3 M KCl (tip resistance 15–30 MΩ), from intact

superfused left atria isolated from mice under inhalation anaesthesia (2.5-4% isoflurane in O_2, 1.5L/min). Voltage signals were amplified (Axoclamp 2B; Molecular Devices, USA), digitized, displayed and analyzed using spike2 software (Cambridge Electronic Design, UK) at 20 kHz sampling frequency. LA were paced at 2× diastolic threshold through bipolar platinum electrodes. After 15 min pacing for equilibration, preparations were paced successively at 1000ms to 80ms. Action potentials were analyzed following 200 beats at each frequency to ensure steady state prior to recording.

Na^+ current recordings in murine left atrial cardiomyocytes and HEK293 cells expressing the human $Na_v1.5$ channel

Murine hearts were removed under terminal anaesthesia and cell isolation was performed as published. For I_{Na} recordings, murine left atrial cardiomyocytes or HEK293 cells stably expressing the human $Na_v1.5$ channel (SB Ion Channels, Glasgow, UK) were superfused at 5ml.min^{-1}, 22±0.5 °C with a solution containing in mM: NaCl 130, CsCl 5, HEPES 10, $CaCl_2$ 1.8, $MgCl_2$ 1.2 and glucose 10, pH 7.4 (CsOH). 100µM $CdCl_2$ was added to block L-type Ca^{2+} currents. Whole cell patch clamp recordings were obtained in voltage clamp mode using borosilicate glass pipettes (tip resistance 1–3 MΩ, pipette solution CsCl 115, NaCl 5, HEPES 10, EGTA 10, MgATP 5, $MgCl_2$ 0.5 and TEA 10, pH 7.2). Na^+ currents were elicited at 100ms steps to -10mV from holding potentials of -100 to -65mV using an Axopatch 1D amplifier (Molecular Devices, USA) and a CED micro1401 driven by Signal v6 (CED, UK).

Standard I_{K1} currents were isolated using 50µM $BaCl_2$ and applying 10mV step depolarisations (500ms) from -120mV to +50mV. For background K^+ current measurements, the external solution contained in mM: NaCl 130, KCl 5.4, $CaCl_2$ 1, $MgCl_2$ 1, HEPES 10, TEA 10, 4-AP 5, glibenclamide (2µM), $BaCl_2$ (100µM), $NiCl_2$ 2 and glucose 5.5 (pH 7.4 with NaOH), to block voltage-gated K^+ and Ca^{2+} channels and I_{K1} and I_{KATP}. Currents were measured in response to a 5s voltage ramp from -80 to 0mV. Background TASK-like K^+ current was isolated with 10mM $BaCl_2$.

Quantitative immunoblotting of atrial tissue. Frozen LA were homogenized in 30 ml of homogenization buffer per gram of tissue (100 mM Tris, pH 7.4, 2 mM sodium vanadate, 5 mM sodium fluoride, 1× protease inhibitor cocktail tablet/50 mL, 4°C). Samples were separated by electrophoresis on a 10% or 15% SDS polyacrylamide gel. Proteins were transferred to PVDF membranes (0.45µm; GE Healthcare, UK) using semidry blotting (Trans-Blot® Turbo™ Transfer System BioRad). Immunoblots were blocked with 5% non-fat milk in PBS-Tween overnight at 4°C. Blots were incubated for 1-1.5 hours at room temperature with primary antibodies raised against: TASK-2 (1:200; Alomone), $K_v1.6$ (1:200; Alomone), Na/K ATPase alpha-1 (1:10000; Milipore, MA, USA), Na/K ATPase alpha-2 (1:5000; Milipore, MA, USA), Na/Ca exchanger 1 (1:1000; Swant, Switzerland), Serca2a (1:5000; Badrilla, UK) and calnexin (1:2000, ab22595 Abcam). Blots were incubated with $Na_v1.5$ antibody (1:200, Alomone) overnight at 4°C. After incubation with HRP-labeled secondary antibodies, blots were developed using enhanced chemiluminescence (Amersham Pharmacia Biotech) on

Odyssey Fc imager (Li-Cor). Calnexin was used as a loading control. Signals from *Pitx2c*$^{+/-}$ LA samples were normalized to wildtype samples signals on the same gels.